Journal of Non-Newtonian Fluid Mechanics, 24 (1987) 31–65
Elsevier Science Publishers B.V., Amsterdam – Printed in The Netherlands

DELAYED DIE SWELL

DANIEL D. JOSEPH

Department of Aerospace Engineering and Mechanics, University of Minnesota, Minneapolis, MN 55455 (U.S.A.)

JOSEPH E. MATTA

Chemical Research, Development and Engineering Center, Aberdeen Proving Ground, Aberdeen, MD 21010 (U.S.A.)

and KANGPING CHEN

Department of Aerospace Engineering and Mechanics, University of Minnesota, Minneapolis, MN 55455 (U.S.A.)

(Received August 21, 1986)

Summary

The experiments reported here establish that there is a general critical condition associated with die swell which we call delayed die swell. This condition is defined by a critical speed which is the area-averaged velocity, the extrusion velocity, at the exit of the pipe when the swell is first delayed. The delayed swell ratio and delay distance first increase for larger, post-critical values of the extrusion velocity; then the increases are terminated either by instabilities or by smoothing. The maximum post-critical velocity at the pipe exit was always greater than the shear wave speed measured on the shear-wave-speed meter. The post critical area averaged velocity at the position of maximum swell before termination was always less than the shear wave speed. There were always points in the region of swelling where the ratio of the local velocity to the shear wave speed, the viscoelastic Mach number, was unity. The swelling of the jet is a nonlinear phenomenon which we suggest is finally terminated either by instability or when the variations of the velocity, vorticity and stress field are reduced to zero by the inward propagation of shear waves from the free surface of the jet. This propagation is generated by discontinuous "initial" data along x in which the prescribed values of velocity at the boundary change from no-slip in the pipe to no-shear in the jet. The measurements raise the possibility that the delay may be associated with a change of type from supercritical to subcritical flow.

0377-0257/87/$03.50

1. Description of delayed die swell

It is easiest to understand what is meant by delayed die swell by examining the photographs exhibited in this paper. A sequential description of the phenomenon is exhibited in photographs shown as Figs. 1.1–1.5. The working fluid is a 9.5% solution of polyisobutylene in decalin (PIB/D, 9.5%). The values of material parameters for this fluid and the other fluids used in our experiments are given in Table 1. The fluid is extruded vertically downward in the direction of gravity. The effects of gravity are the same in all experiments and are important in downstream regions away from the exit where data were taken. The nozzle diameter d is 1 mm and the length of the capillary tube is 6.125 cm.

The local velocity $\boldsymbol{u}(x, r) = (u, w)$ where u is the axial and w the radial component, $\bar{u}(x)$ is the area averaged velocity and $\bar{u}(0)$ is the average velocity at the pipe exit. The diameter of maximum swell at $x = L$ is D and the swell ratio is D/d.

Figure 1.1 shows the jet under pre-critical conditions, before the delay. The swell ratio increases with $\bar{u}(0)$ to 3.83. Figure 1.3 shows the jet after the delay has commenced $\bar{u}(0) > u_c$. Figure 1.2 shows the jet at criticality $\bar{u}(0) = u_c$. Figures 1.3 and 1.4 show what happens as the extrusion velocity $\bar{u}(0)$ is increased. First D increases with $\bar{u}(0)$, then near $\bar{u}(0) = 1519$ cm/s, D begins to decrease. The configurations shown in Figs. 1.1–1.3 appear to be steady. There is evidently a point of instability at $\bar{u}(0) = 1012$ cm/s which leads to an oscillation in which the point of delay moves between extreme values. The maximum and minimum delay distance over a cycle is shown for $\bar{u}(0) = 1519$ cm/s in Fig. 1.5(a) and 1.5(b).

Figures 1.1–1.5 show delayed die swell in a dramatic form. In general the delay starts in a less dramatic way; a point of inflection in the swell profile suddenly appears at the pipe exit when the extrusion velocity is raised above a critical value. The strength of the delay varies widely over different fluids.

The dynamics of die swell is not well understood and delayed die swell is perhaps less well understood. However, there is an apparent connection

Fig. 1.1. Extrusion of PIB/D, 9.5% under pre-critical conditions: $[d, \bar{u}(0), D] = [1$ mm, 404 cm/s, 3.33 mm$]$.

Fig. 1.2. Extrusion of PIB/D, 9.5% at criticality: $[d, \bar{u}(0), D] = [1$ mm, 785 cm/s, 3.83 mm$]$.

Fig. 1.3. Extrusion of PIB/D, 9.5% under post-critical conditions: $[d, \bar{u}(0), D] = [1$ mm, 934 cm/s, 4.17 mm$]$.

Fig. 1.4. Unsteady extrusion of PIB/D, 9.5% under post-critical conditions. The oscillation has just commenced. $[d, \bar{u}(0), D] = [1$ mm, 1214 cm/s, 4.5 mm$]$.

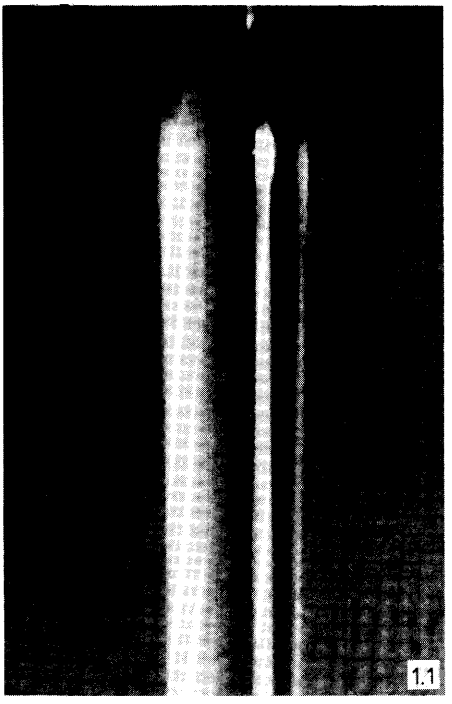
1.1

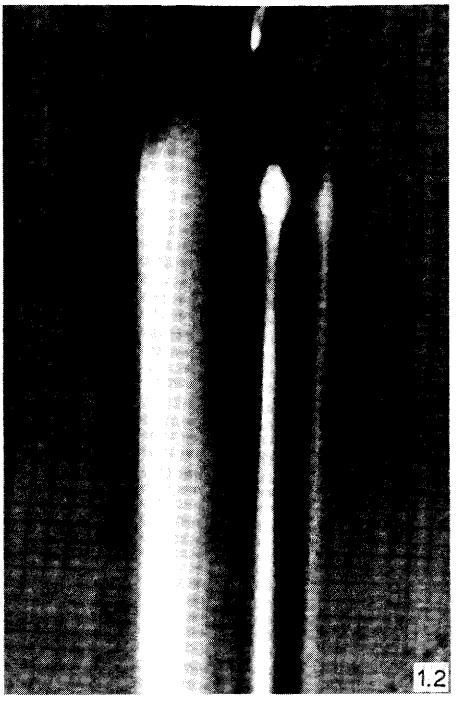
1.2

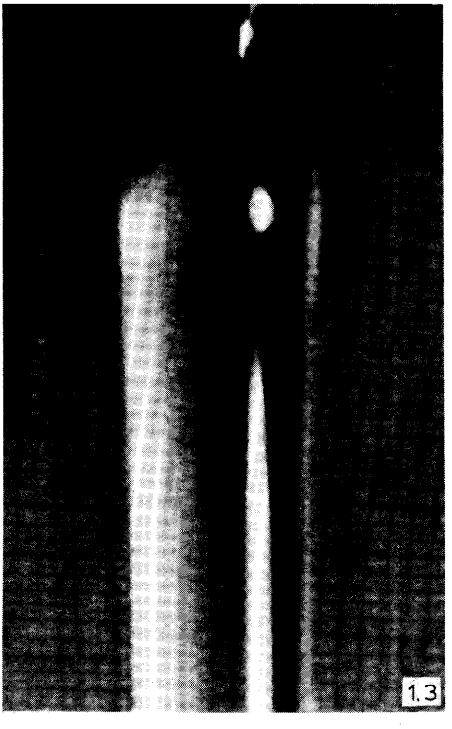
1.3

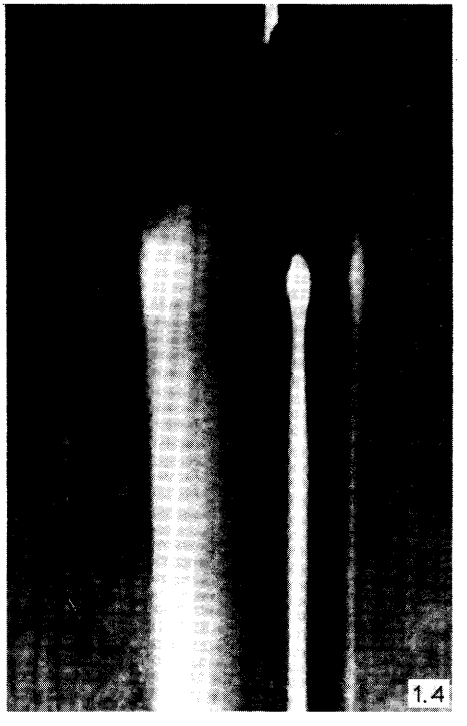
1.4

TABLE 1

Values of material parameters at $23 \pm 1°C$

Liquid	Density ρ(g/cc)	Viscosity $\tilde{\mu}$(Pa-s)	Wave speed c(cm/s)	Rigidity Gc(Pa)	Relaxation time $\tilde{\mu}/Gc$(s)
AP30, 1%	1.16	53.80	30.7	109.33	0.4921
AP30, 1.5%	1.17	160.0	38.4	172.52	0.9274
CMC, 1%	1.19	44.76	50.6	304.68	0.1468
CMC, 1.2%	1.20	84.48	57.0	389.88	0.2167
CMC, 1.3%	1.21	129.8	81.0	793.88	0.1628
ELVACITE, 9.8%	1.05	0.90	67.0	471.35	0.0019
K-125, 5%	1.08	1.10	45.4	222.61	0.0049
PIB/D, 6%	0.90	11.01	90.1	730.62	0.0151
PIB/D, 9.5%	0.91	139.0	162.0	2204.5	0.0631
PIBM, 1%	0.93	0.065	18.8	32.87	0.0020
PIB/T, 4%	0.87	0.87	53.5	249	0.0035
PIB/T, 5.5%	0.88	5.44	60.6	323.2	0.0168
PIB/T, 6%	0.89	41.0	115.0	1177.0	0.0348
PMMA, 1%	1.06	0.20	17.9	33.90	0.0059
PMMA, 2%	1.07	13.0	25.0	66.94	0.1194
POLYOX, 1.3%	1.00	11.9	24.7	61.01	0.1950
POLYOX, 2.5%	1.01	203.3	51.2	264.77	0.7679

between various critical values of the velocities associated with the delay and the shear wave speed we measure using a wave-speed meter [1]. This connection obliges us to try to determine ways in which wave propagation might be important in die swell and in delayed die swell. The critical speeds in delayed die swell are also such that the flow in the pipe may have regions in which hyperboliticity is important (cf. Ahrens, Yoo and Joseph [2], in this issue). This suggests that delayed die swell may have some features in common with other problems governed by PDE's of mixed type.

2. Previous work on delayed die swell

Many casual photographs of die swell under subcritical conditions have been published in the last fifty years. Photographs of delayed die swell have appeared in the literature less frequently. We know of photographs of Merrington [3], Giesekus [4], Metzner, White and Denn [5], Middleman [6] and Brenschede and Klein [7]. Among these authors only Giesekus followed by Brenschede and Klein have noted that delayed die swell is a critical phenomenon. Their explanation is a molecular one which involves the precipitation of polymer. We think this explanation cannot explain that the delay is a general property independent of the nature of solute and solvent

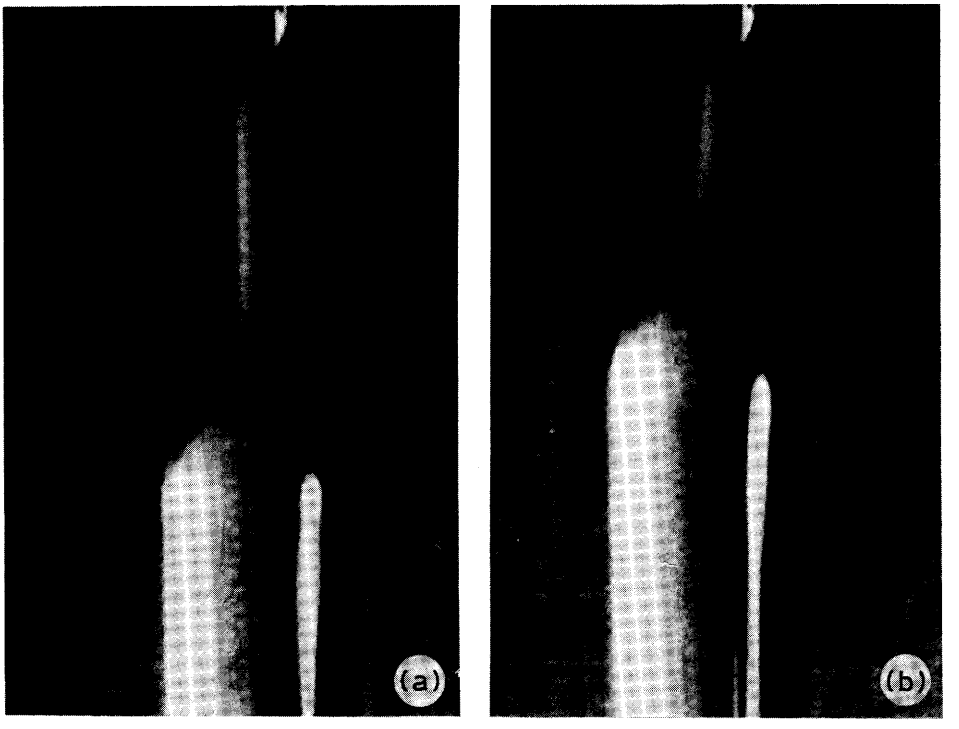

Fig. 1.5 Unsteady extrusion of PIB/D, 9.5% under post critical conditions: $[d, \bar{u}(0), D] = \{1$ mm, 1519 cm/s, 3.92 mm]. (a) shows the maximum and (b) the minimum delay on one cycle.

and is not consistent with other observed properties reported in this paper. Joseph [8] noted that "the delayed die swell seems to occur at a critical speed, not so different as one might expect from a change of type. Of course, the reason for the delayed swell is not understood. The form of the jet reminds one of a hydraulic jump which is the shock phenomenon corresponding to shocks in gas dynamics."

This is the first paper to report systematic experiments which look at delayed die swell. We found that the delay is a critical phenomenon, that it is a general phenomenon which occurred in all seventeen solutions tested by us and that there is a relation between die swell and relaxation through wave propagation.

3. Notations

To prepare for our discussion it is useful to define certain quantities. Many of these quantities are exhibited in Fig. 3.1.

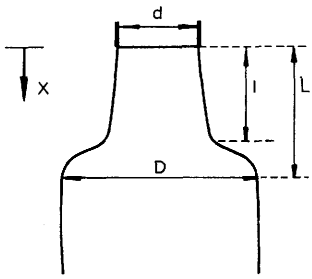

Fig. 3.1. Sketch of delayed die swell. Q is the volume flow rate constant throughout the jet. $\bar{u}(x)$ is the area averaged velocity; $\bar{u}(0) = Q/\pi a^2$ where $a = d/2$ is the radius of the pipe. The delay distance is l. The distance to the maximum swell is L.

List of symbols

ρ density (g/cm^3)
$\tilde{\mu}$ static or zero shear rate viscosity (Pa-s)
c speed of vorticity waves (shear waves) into a fluid at rest (or rigid motion) (cm/s)
G_c effective rigidity, $G_c = \rho c^2$(Pa)
$\bar{\lambda}$ mean relaxation time, $\bar{\lambda} = \tilde{\mu}/G_c$ (s)
R Reynolds number at the pipe exit based on static viscosity, $R = \rho d\bar{u}(0)/\tilde{\mu}$
ϕ Shear rate at the pipe exit, $\phi = 8\bar{u}(0)/d$
D/d Swell ratio
L Terminal swell distance. $x = L$ is position where D is maximum.
l delay distance
$\bar{u}_c$ $= \bar{u}_c(0) = Q_c/\pi a^2$ Mean velocity at the flow rate of incipient delay. There is a delayed die swell when $Q > Q_c$.
M_0 $= U/c$ Viscoelastic Mach number at exit $x = 0$
U $= 2\bar{u}(0)$ Definition of U, this is an approximation of the center line velocity at exit which is exact when the profile at exit is parabolic.
M_c $= U_c/c$ $(U_c = 2\bar{u}_c(0))$ Viscoelastic Mach number at criticality
$M(L) = \bar{u}(L)/c$ Viscoelastic Mach number at the point of termination of the swell. It may be assumed the velocity $u(L, r) = \bar{U}(L)$ is uniform at the point of maximum swell.

4. Experiments

Two devices were used to extrude the test liquids, a controlled displacement device at the University of Minnesota and a controlled pressure device at the Aberdeen Army Laboratory. Results obtained from the two devices are consistent with one another.

The first device was a piston–cylinder apparatus in which the piston velocity could be accurately controlled by a microprocessor (manufactured commercially by MTS, Materials Testing System). The flow rate Q in the capillary can be determined from the rate of advance of the piston in the cylinder. The inner diameter of the capillaries were 0.81, 1, 1.57, 2.08 and 3.175 mm respectively. The length/diameter ratio for these capillaries was greater than thirty. The smallest and largest nozzles were late additions in our experiments.

The second device employs pressurized nitrogen to force the stored fluid from a 600 ml reservoir vertically downward through a 15 cm long capillary that extended 2 cm up into the reservoir. Capillaries with various inner diameters were used: 2.39, 1.81, 1.7 and 1.25 mm. When pressurized the fluid extruded vertically downward from the orifice and was collected in a sample cup placed about 10 cm below the nozzle tip. The average velocity was determined by weighing fluid extruded in a certain interval of time.

All of the delayed swell data on both devices, except the data exhibited in Section 8, were taken on a Spin Physics high speed video and motion analysis system. The critical condition for delayed swell was determined by iteration of visual observations on the video from above and below. The critical condition is very sharp and it is possible to determine it with good accuracy. The same method of iterative determination of critical conditions was made on the pressurized system, by monitoring the gauge pressure iteratively around the critical condition. The reticule feature on the video system allows for accurate measurements of the delay distance, swell ratio and shock layer thickness. Most of the photographs shown in this paper are taken by photographing the video screen with a polaroid camera.

The static viscosities were measured on a standard cone-and-plate rheometer and the wave speeds with the wave speed meter. Material properties of test liquids are exhibited in Table 1.

5. Shear wave speeds and effective moduli

The interpretation of the observations of delayed die swell may require that one first understands some properties of wave propagation. Fluids which possess instantaneous and relaxing elasticity, Maxwell models, BKZ models with smooth kernels, Doi–Edwards models and more generally fluids which satisfy the mathematical hypotheses of the type of theory of fading memory of Coleman and Noll [9] admit the propagation of shear waves. Fluids which also possess a purely viscous term or its equivalent exhibit viscous diffusion, smoothing waves. Jeffrey's model, Oldroyd's model B, the Curtiss–Bird models (with $\epsilon \neq 0$) and more generally all fluids which

satisfy certain of the mathematical hypotheses of the theory of fading memory of Saut and Joseph [10] possess some elasticity, with viscous diffusion, smoothing waves.

For motions which perturb rest, the extra stress τ is given by a generalization of Boltzmann's equation of linear viscoelasticity

$$\tau = 2\mu \boldsymbol{D}[\boldsymbol{u}(\boldsymbol{x}, t)] + 2\int_0^\infty G(s)\boldsymbol{D}[\boldsymbol{u}(\boldsymbol{x}, t-s)]\, \mathrm{d}s, \tag{5.1}$$

where $\boldsymbol{D}[\boldsymbol{u}]$ is the symmetric part of the $\boldsymbol{x}$ gradient of $\boldsymbol{u}$, $G(s)$ is a smooth, decreasing (to zero) kernel, called the shear relaxation function, and μ, the Newtonian viscosity, is associated with viscous diffusion. The value $G(0)$ is called the rigidity or shear modulus. When $\mu = 0$, the fluid has instantaneous and relaxing elasticity and admits wave propagation. This propagation can be associated with waves of vorticity; the vorticity equation is hyperbolic [11,12]. The vorticity wave is a shear wave when the problem has only one space dimension. The speed c of the wave of vorticity is given by

$$c = \sqrt{G(0)/\rho}\,, \tag{5.2}$$

where ρ is the density of the fluid. The formula (5.2) has been known since the early 1950's, at least.

Hidden in (5.1) is the notion of an effective viscosity and an effective modulus or rigidity. When (5.1) is evaluated for steady shearing, the zero-shear or static viscosity $\tilde{\mu}$ is given by

$$\tilde{\mu} = \mu + \eta, \tag{5.3}$$

where the elastic viscosity

$$\eta = \int_0^\infty G(s)\, \mathrm{d}s \tag{5.4}$$

is the area under $G(s)$. It is not difficult to measure $\tilde{\mu}$, but reliable methods for measuring μ and η are not known. There is a fundamental problem which is discussed by Joseph, Narain and Riccius [13]. Even though the Newtonian viscosity μ is probably zero in all fluids, there can be an effective viscosity μ which is associated with the decay of short lived elastic modes. In the first instant, the response of a fluid to impulsive data is completely elastic. This corresponds to a response governed by (5.1) with $\mu = 0$. At large times, after $G(t)$ has decayed to a negligible value the response is purely viscous, with viscosity η. At intermediate times t_0, $G(t_0)$ has relaxed some but is not yet surpassingly small. The dynamic effects of relaxed modes are equivalent to a viscosity which is approximately equal to the area under $G(t)$ for $0 \leqslant t \leqslant t_0$. We can choose different effective relaxation functions $G_\mu(t)$ and effective viscosities μ with $G_\mu(t) = G(t)$ for $t > t_0$ which have the

same response as the true $G(t)$ for $t > 0$. We only require that the past response of all these different representations give rise to the same viscous response in the future; i.e.,

$$\mu + \int_0^{t_0} G_\mu(t)\, dt = \int_0^{t_0} G(t)\, dt. \tag{5.5}$$

The decomposition of $G(t)$ into an effective relaxation function and viscosity is not unique.

If we could know $G(t)$ for all $t \geqslant 0$, there would apparently be no reason to introduce an effective viscosity and relaxation function. In fact, there are certain good reasons for introducing $\mu \neq 0$, even though $\mu = 0$. These reasons center on the smoothing properties associated with fluids with $\mu \neq 0$. (See Joseph and Saut [12] for a fuller discussion of these issues.)

We cannot find $G(t)$ for small values of t because our rheometers have non-zero response times. In most, perhaps all, fluids the values of $G(t)$ are extremely large when t is small enough (we are thinking of $t < 0.001$ s). It makes sense to model this unknown early part of the relaxation function with an equivalent (but equally unknown) viscosity. In ordinary applications we do not see the earliest responses which go by too fast, so that the early large values of $G(t)$ enter these applications only as an effective viscosity.

The following construction of an effective moduli can be considered (see Fig. 1 of Joseph, Narain and Riccius [13]). We first determine $G(t)$ for $t \geqslant t_0$, where t_0 is as small as rheometry will allow. We choose $G_\mu(0) = G(t_0)$ and drop a tangent to $G(t)$ at $t = t_1$ from the point $[0, G_\mu(0)]$. Then

$$G_\mu(t) = \begin{cases} G_\mu(0) - \left[G_\mu(0) - G(t_1)\right] t/t_1, & 0 \leqslant t \leqslant t_1, \\ G(t), & t \geqslant t_1, \end{cases} \tag{5.6}$$

and

$$\mu = \int_0^{t_1} \left[G(t) - G_\mu(t)\right] dt.$$

The function $G(t)$ is expected to be rapidly decreasing from values as high as $G(0) = 10^9$ Pa for small t, say $t < 10^{-7}$ s. This rapid decrease is associated with the fast relaxation times of small molecules. The larger molecules relax more slowly so that it is conceivable that $G_\mu(0) = G(t_0)$ is not sensitive to changes in t_0 which are small relative to the slowest relaxation time for the macromolecules.

Joseph, Riccius and Arney [1] measured the wave speed c on the wave-speed meter and computed the effective rigidity $G_\mu(0) = G_c = \rho c^2$ where $c = \delta/T$, δ is gap size and T is a measured transit time for a signal to travel across the gap. The value of c is independent of the gap size, more or less, and is consistent with standard rheological data.

TABLE 2

List of test liquids

β	Percent by weight of the polymer in solution
DEM	Diethylmalonate is the solvent used with PMMA, K-125 and ELVACITE
AP-30, β	Separan, Polyacrylamide in 50%$-\beta$ water, 50% glycerin ($\beta = 1\%$, 1.5%)
CMC, β	Carboxymethylcellulose in 50%$-\beta$ water, 50% glycerin ($\beta = 1\%$, 1.2%, 1.3%)
ELVACITE, β	Polymethyl/methacrylate, 4×10^5 molecular weight, in DEM ($\beta = 9.8\%$)
K-125, β	A copolymer of 80% PMMA and 20% poly(ethyl/butyl acrylate) with a 1.9×10^6 viscosity molecular weight ($\beta = 5\%$)
PIBM, β	Polyisobutyl methacrylate, 5.5×10^6 molecular weight, in bis (2-ethyl-hexyl) hydrogen phosphite (BIS-2)($\beta = 1\%$)
PIB/D, β	Polyisobutylene in Decalin ($\beta = 6\%$, 9.5%)
PIB/T, β	Polyisobutylene in Toluene ($\beta = 4\%$, 5.5%, 6%)
POLYOX, β	Polyethylene oxide (WSR 301) in water ($\beta = 1.3\%$, 2.5%)
PMMA, β	Polymethyl methacrylate, 6×10^6 molecular weight, in DEM ($\beta = 1\%$)

We used the wave-speed meter to measure c for the seventeen test liquids listed in Table 2. The wave speeds are listed in Table 1; they vary over a decade, from 17.9 to 162 cm/s.

The remarkable connection between the wave speed and delayed die swell may be described as follows: Let $U(x)$ be the maximum value of the velocity $U(x, r)$ over the cross section at x. Suppose that $U(0) = 2\bar{u}(0)$ where $\bar{u}(0)$ is the area average of $u(x, r)$ at the nozzle exit $x = 0$. Because of shear thinning, $U(0) = \alpha\bar{u}(0)$, $1 < \alpha \leqslant 2$, so we are a little high, but less high when the nozzle diameter is larger and the shear rate is smaller. Suppose further that after the swell the velocity in the jet is uniform. Then we found that the maximum velocity was always (nearly always, see Fig. 6.3) supercritical

$$U(0) \geqslant c \tag{5.7}$$

before the swell and subcritical

$$\bar{u}(L) < c \tag{5.8}$$

after the swell, at $x = L$. The forward velocity of some point in the region of swelling is c.

These observations suggest that delayed die swell may be associated with a change in type. For Maxwell models the change of type is a change in the type of the second order equation governing the vorticity. The problem of change of type for the flow in the pipe is analyzed for an upper convected Maxwell model in the paper by Ahrens, Yoo and Joseph in this issue. Other problems which involve a change of type have been considered by Rutkevich [14,15], Ultman and Denn [16], Luskin [17], Joseph, Renardy and Saut [11],

Joseph [8], Yoo and Joseph [20], Yoo, Ahrens and Joseph [18], Dupret and Marchal [19] and Joseph and Saut [12].

If we assume that the velocity at exit is fully developed, then

$$u(0, r) = U(0)(1 - 4r^2/d^2) \tag{5.9}$$

and the vorticity ζ is given by

$$\zeta(0, r) = \frac{-\partial u(0, r)}{\partial r} = \frac{8rU(0)}{d^2}. \tag{5.10}$$

It is perhaps useful to associate die swell with the relaxation of the developed distribution (5.10) at exit to zero downstream where the flow is uniform. This relaxation is induced by a discontinuous prescription of the data, no slip on the wall ($r = d/2$), no shear at the surface of the jet. This prescribed discontinuity gives rise to an integrable lip singularity in the stress and pressure when the fluid in Newtonian. It is probable that the prescribed discontinuity gives rise to singular behavior when the fluid is non-Newtonian. In any event the discontinuous prescription of the boundary data requires that the flow readjust from pipe flow with a linear vorticity profile (5.10) at exit to a uniform flow with zero vorticity downstream. This readjustment is powered by waves which carry the boundary data into the jet. In general the speed of such waves at each point depends on the state of stress there, but $c = \sqrt{G(0)/\rho}$ in all motions perturbing rigid ones and in shearing motions of all amplitudes in one space dimension of upper convected Maxwell fluids. The vorticity in the pipe is greatest at the wall and is zero at the center of the pipe and downstream where the flow is uniform. The vorticity at the boundary is impulsively reduced to zero at the exit lip and the region of zero vorticity consumes more and more of the jet as x increases.

We could imagine the relaxation to zero of all of the vorticity in the jet is accomplished in a distance L at a time τ and that there is a velocity $\hat{u} < \bar{u}(0)$ such that $L \approx \hat{u}\tau$. At this time and place the wave of relaxation has penetrated all the way to $r = 0$, a distance $D/2$. The speed of penetration might be estimated as $w = c - \hat{v}$ where $\hat{v}$ is the outward velocity of particles which could itself be estimated $\hat{v} \approx (D - d)/\tau$. This gives $D/2 \approx w\tau$ and

$$\frac{2L}{D} \approx \frac{\hat{u}}{w} = \frac{\hat{u}}{c - \hat{v}}. \tag{5.11}$$

The usual way to estimate relaxation times uses data for the first normal stress. This might be good for the die swell application, since the swelling is associated with normal stresses, especially with excess tension. We do not have the rheological data for this estimate. The mean relaxation time $\bar{\mu}/G_c$ could also be used for τ, but it seems to be smaller than the time which is

actually effective in the dynamics of swelling. We always get $\hat{u} < \bar{u}(0)$ when $\bar{\lambda} = \tau$, and the estimate (5.11) is also in rough agreement with measured data when $\bar{u}(L) \leqslant \hat{u} < \bar{u}(0)$.

The considerations of the previous paragraph apply to pre-critical and post-critical flows and they do not explain the delay. The analysis of Ahrens, Yoo and Joseph [2] of hyperbolicity and change of type for flows perturbing developed flow in a pipe is possibly relevant for delayed die swell. A defect of that analysis is that it holds surely only for the special constitutive equation associated with the upper convected Maxwell model. For this nonlinear model the vorticity equation is either elliptic or hyperbolic, and it may be hyperbolic in some regions of flow and elliptic in others. If $U > c$ there is a region in the center of the pipe in which the vorticity equation is hyperbolic; outside of this region the vorticity equation is elliptic. The region of hyperbolicity is very small under the condition of high elasticity number, characteristic for our experiments.

The question is: can there be an important hyperbolic region in the jet outside the pipe? An affirmative, though speculative, answer can be framed along the following line. The equation for flows perturbing uniform flows are hyperbolic everywhere that $U > c$, and in three-dimensional flows they give rise to the Mach cones described in the appendix of the paper by Ahrens, Yoo and Joseph [2]. When a fluid is extruded at high speed from a pipe, the center line velocity $U \gg c$, but $u(x, r)$ vanishes at the exit lip $(x, r) = (0, d/2)$. The velocity at the surface $r = R(x)$ of the jet accelerates rapidly and if U were large enough the surface velocity would exceed c already for small values of $x > 0$. The velocity profiles for these values of x may not be too different than uniform ones, locally at each x. At the very least, we might expect that each and every value of the velocity on the cross section of the delay would be greater than c, with an associated hyperbolic vorticity equation.

6. Values of parameters at criticality

Delayed die swell seems to be a general phenomenon in elastic liquids. We found a robust and reproducible critical condition for delay in each and every one of the seventeen test fluids measured at the University of Minnesota. The existence of delay is less apparent in fluids of small viscosity and time of relaxation. The 1% solutions of PMMA and PIBM are in this category. These fluids are close to a Newtonian limit and considerable smoothing, probably viscous smoothing, is evident in the photographs of the delay shown in Figs. 8.1–8.4. We could not determine a die swell or a delay in soybean oil. This oil is Newtonian by reputation but appears to have a definite wave speed and shear modulus [1].

The flow at criticality can be steady or unsteady. This property of the critical flow evidently depends only on the fluid and not on the experiment. Flows which were unsteady in the constant flow rate apparatus were also unsteady in the constant pressure gradient apparatus. The flows which were unsteady at criticality are listed in Table 3. In Figs. 6.1 and 6.2 we have exhibited photographs of unsteady delayed die swell in an aqueous solution of 1.5% AP30. The unsteady flows sometimes emerge at an angle from the axis of the nozzle. The sidewise deviation from the vertical rotates around the axis of the pipe. We could not eliminate unsteadiness from the flows in which it occurred. We do not know why some fluids give rise to unsteady flow at criticality and some do not. Fluids with the longest mean times of relaxation (Table 1) were unsteady at criticality.

The Tables 3 and 4 we have listed the measured values of swell parameters at criticality. The values of c for different fluids are given in Table 1. Critical Reynolds number (based on the static viscosity) and critical shear rates can be computed from these tables. The critical swell ratio D/d, terminal swell distance ratio L/d and the terminal value $\bar{u}(L)/c$ of the viscoelastic Mach number are not well defined when the flow is unsteady. The values given in Table 3 are average values over one cycle. Since the flow rate is accurately prescribed, $\bar{u}(0)$ is steady. The unsteady flow appears to arise as an instability.

Several conclusions follow from inspection of Tables 3 and 4.

(1) The critical velocity $\bar{u}_c$, the swell ratio D/d and the terminal swell distance ratio L/d are decreasing functions of d, the pipe diameter.

(2) The critical Mach number at exit, $M_c = U_c/c$, $U_c = 2\bar{u}_c$ were nearly always larger than one. (The value $M_c = 0.954$ for 1.3% CMC was the only exception.)

TABLE 3

Critical parameters for delayed die swell when the flow at criticality is unsteady

Polymer solution	d (mm)	$\bar{u}(0)/c$	L/d	D/d	$\bar{u}(L)/c$	Fig.
AP30, 1%	1	3.989	2.3333	2.8333	0.4970	
AP30, 1.5%	1	4.477	4.3333	3.3333	0.4030	6.1
POLYOX, 1.3%	1	3.975	3.6667	3.4167	0.0292	
POLYOX, 2.5%	0.81	2.899	2.7692	3.4615	0.2419	
	1	2.283	2.6154	3.3846	0.1993	
	1.57	1.342	1.9600	2.5200	0.2144	
	2.08	0.879	1.4848	2.0000	0.2198	
	3.175	0.5491	1.4359	1.9231	0.1485	
PMMA, 2%	2.39	7.6000	2.5000	3.2222	0.8055	

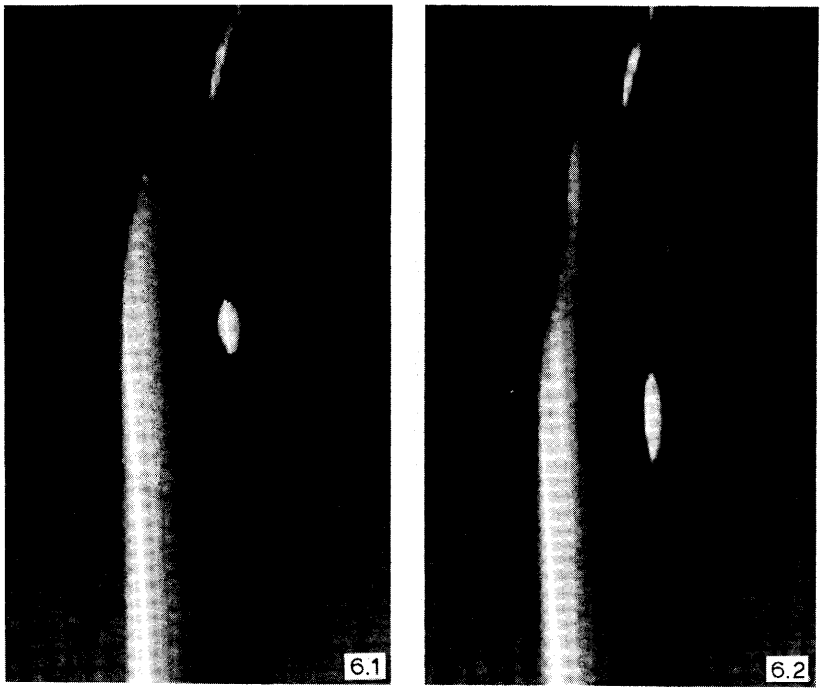

Fig. 6.1. Die swell in AP 30, 1.5% ($c = 38.4$ cm/s) at criticality $\bar{u}(0)/c = 4.48$. The pipe diameter is 1 mm. The extrusion velocity $\bar{u}(0)$ is steady but the flow is generally unsteady. The downstream value $\bar{u}(L)/c$ at the point $x = L$ of maximum swell is 0.40.

Fig. 6.2. Post-critical die swell: $\bar{u}(0)/c = 6.565$ and $\bar{u}(L)/c < 1$. The flow is unsteady and downstream quantities like L, D, M, l depend on t, are oscillating.

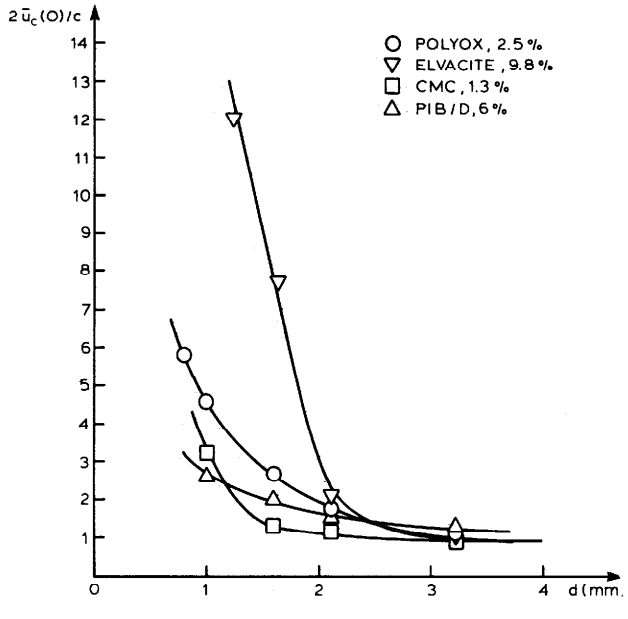

Fig. 6.3. Critical Viscoelastic Mach number based on the approximation $2\bar{u}_c$ of the center line velocity at exit as a function of nozzle diameter.

TABLE 4

Critical parameters for delayed die swell when the flow at criticality is steady

Polymer solution	d (mm)	$\bar{u}(0)/c$	L/d	D/d	$\bar{u}(L)/c$	Fig.
PIB/T, 4%	1	0.8042	0.6429	1.6429	0.2979	
PIB/T, 5.5%	1	1.1341	0.9231	2.0769	0.2629	
PIB/T, 6%	1	2.2121	1.0000	2.3330	0.4045	
CMC, 1%	1	2.1400	1.0000	1.9170	0.5823	
K-125, 5%	1	2.2444	2.8333	3.7500	0.1596	
PIB/D, 6%	1	1.2869	2.0000	3.3636	0.1138	7.4
	1.57	0.9790	1.7950	2.8952	0.1168	
	2.08	0.7437	1.3986	2.4039	0.1287	
	3.175	0.7147	1.2312	1.8898	0.2002	7.1
PIB/D, 9.5%	1	4.6795	1.8333	3.8333	0.3185	1.2
CMC, 1.2%	1.25	2.0702	0.8750	1.6250	0.7831	
	2.39	1.7544	0.5926	1.5000	0.7789	
ELVACITE, 9.8%	1.25	5.9701	1.5000	2.4500	0.9728	
	1.76	3.9254	1.2500	2.1875	0.8024	
	2.08	0.9798	1.5769	2.3077	0.1840	
	3.175	0.5046	1.0000	1.7500	0.1648	
CMC, 1.3%	1	1.5970	0.9167	2.0833	0.3680	
	1.57	0.6273	1.0616	1.9639	0.1626	7.11
	2.08	0.5875	0.8413	1.8429	0.1730	
	3.175	0.4772	0.7087	1.5748	0.1924	7.8

(3) There seems to be a limiting value of M_c for large values of d. The evidence for this conclusion is exhibited in Fig. 6.3. This figure is not inconsistent with a limiting value $M_c = 1$, but there are too few data to make a certain statement.

(4) Whenever the die swell is delayed, there are points on the exist plane where $u(0, r) = c$.

(5) The critical terminal Mach number, after the swell $M(L) = \bar{u}(L)/c$, is always definitely less than one.

The data here, and in section 7, are not consistent with a brutal analogy between delayed die swell and hydraulic jumps. The velocity $\bar{u}(0)$ at the exit can be much larger than c in pipes of small diameter even under pre-critical conditions. It is likely that the speed c of vorticity waves in regions of uniform or rigid motion is not the relevant wave speed in the very stressed region at the exit of a pipe of small diameter. We also did not rule out the possibility that there is a fluid and a pipe of large diameter such that delayed die swell can occur with $U < c$. (The exception mentioned under (2) above may or may not realize this possibility.)

7. Post-critical values of the flow parameters

More energy is put into the flow as the extrusion velocity $\bar{u}(0)$ is increased. The delay distance increases with $\bar{u}(0)$ and the swell ratio first increases, then decreases with $\bar{u}(0)$. The shape of jets with delayed swells differs from fluid to fluid. More dilute solutions, with smaller times of relaxation have rather smooth transitions as might be expected of fluids with a large Newtonian viscosity (see Figs. 8.1–8.4). The Separan and Polyox solutions have a slight swell at exit followed by a large delayed swell (see Fig. 6.2). In general the small diameter of the jet downstream from the delay increases slightly with distance and abruptly at the point $x = l$ of maximum delay.

There is no possibility for the delay to persist. It must eventually be destroyed by the viscous action of decayed elastic modes or by the stretching effects associated with the acceleration of gravity.

We took data for increasing values of $\bar{u}(0) > \bar{u}_c$ in the post-critical region. The delay distance increases monotonically from zero at $\bar{u}(0) = \bar{u}_c$. The swell first increases, or does not decrease, then decreases as $\bar{u}(0)$ is increased. The taking of data was terminated at a certain $\bar{u}(0)$ for three different reasons.

(1) We did not wish to extend the rated capacity of the transducer on the constant displacement extruder.

(2) A flow instability intervened and we could not measure unique values of the delay distance or swell ratio. An example of this instability is shown in Figs. 1.5, 7.7, 7.14 and 7.15.

(3) The swell ratio showed marked decreases and the swell region was smoothed. Examples of this type of smoothing are shown in weak form in Fig. 7.17 and in strong form in Fig. 8.

In those cases in which we can identify a definite l and a definite L we may speak of a shock layer transition. This is the region of thickness $L-l$ in which there is a sharp change in the radius of the jet. There are many cases in which a shock layer may be easily identified, there are marginal cases and cases in which the identification of such a layer is not possible. This definition of a shock layer holds under pre-critical conditions, but we do not look for shock-like transitions in the pre-critical case. We are introducing the notion of shock layers for the post-critical case, in which there is a delay, $l > 0$. Tables 5–18 summarize our results in the post-critical case.

The post-critical case is defined by $\bar{u}(0) > \bar{u}_c$. The following conclusions are evident from the entries in the tables.

(1) $l > 0$ increases with $\bar{u}(0)$.

(2) $M_0 = 2\bar{u}(0)/c > 1$.

(3) $M(L) = \bar{u}(L)/c$ is an increasing function of $\bar{u}(0)$.

TABLE 5

Measured values of flow parameters under post-critical conditions for CMC/1%, $d = 1$ mm

$\bar{u}(0)/c$	l/d	L/d	D/d	$\bar{u}(L)/c$
2.1400	0.0000	1.0000	1.9170	0.5823
2.3400	0.1670	1.0000	1.9170	0.6368
2.4960	0.1670	1.1670	2.0000	0.6240
2.6740	0.1670	1.1670	2.0000	0.6685
2.9950	0.4170	1.2500	2.0000	0.7488
3.7440	a 1.4167	2.5000	1.8333	1.1140
	b 1.5833	2.8333	1.7500	1.2225

TABLE 6

Measured values of flow parameters under post-critical conditions for CMC/1.3%, $d = 1$ mm

$\bar{u}(0)/c$	l/d	L/d	D/d	$\bar{u}(L)/c$
1.5400	0.0000	0.9167	2.0833	0.3548
1.5900	0.0000	0.9167	2.0833	0.3680
1.6585	0.0833	0.9167	2.1667	0.3533
1.7248	0.2500	1.0000	2.1667	0.3674
1.7967	0.2500	1.1667	2.0833	0.4140
1.8748	0.3333	1.5000	2.0833	0.4320
1.9600	0.7500	1.6667	2.0833	0.4516
2.0533	1.0833	2.0000	2.1667	0.4374
2.1560		3.0833	1.7500	0.7040
3.3157			1.0833	2.8254

TABLE 7

Measured values of flow parameters under post-critical conditions for CMC/1.3%, $d = 1.57$ mm

$\bar{u}(0)/c$	l/d	L/d	D/d	$\bar{u}(L)/c$
0.5855	0.0000	1.0616	1.9639	0.1518
0.6273	0.0000	1.0616	1.9639	0.1626
0.6755	0.1592	1.1146	1.9639	0.1752
0.7318	0.3715	1.1146	2.0170	0.1799
0.7984	0.5839	1.4862	2.1231	0.1771
0.8782	1.0616	1.9639	1.9107	0.2405
0.9758	1.8046	2.9724	1.8046	0.2996
1.0978			1.4862	0.4970

TABLE 8

Measured values of flow parameters under post-critical conditions for CMC/1.3%, $d = 2.08$ mm

$\bar{u}(0)/c$	l/d	L/d	D/d	$\bar{u}(L)/c$
0.4993	0.0000	0.7612	1.7227	0.1683
0.5875	0.0000	0.8413	1.8429	0.1730
0.6658	0.2003	1.1619	1.9231	0.1800
0.7682	0.6410	1.4023	1.8830	0.2167
0.8322	1.0016	1.8029	1.8830	0.2347
0.9079	1.3622	2.3237	1.8029	0.2793
1.0234		3.3654	1.5625	0.4192

TABLE 9

Measured values of flow parameters under post-critical conditions for CMC/1.3%, $d = 3.175$ mm

$\bar{u}(0)/c$	l/c	L/d	D/d	$\bar{u}(L)/c$
0.2147	0.0000	0.4724	1.2861	0.1298
0.2684	0.0000	0.4987	1.3648	0.1441
0.3068	0.0000	0.6299	1.4173	0.1527
0.3904	0.0000	0.6299	1.4698	0.1807
0.4772	0.0000	0.7087	1.5748	0.1924
0.5368	0.0787	0.8136	1.6535	0.1964
0.6135	0.2362	0.9711	1.6535	0.2244
0.7158	0.8924	1.6273	1.5748	0.2886

TABLE 10

Measured values of flow parameters under post-critical conditions for K-125/5%, $d = 1$ mm

$\bar{u}(0)/c$	l/d	L/d	D/d	$\bar{u}(L)/c$
1.8123	0.0000	1.7500	3.6667	0.1349
1.9078	0.0000	2.6667	3.5833	0.1486
2.0000	0.0000	2.5833	3.6667	0.1488
2.1197	0.0000	2.5833	3.6667	0.1577
2.2444	0.0000	2.8333	3.7500	0.1596
2.3847	0.3333	2.9167	3.7500	0.1696
2.5385	0.4167	3.3333	3.8333	0.1728
2.7198	0.5833	3.5000	4.0000	0.1700
2.9290	1.1661	4.1667	4.0000	0.1831
3.1731	2.2500	6.3333	4.3333	0.1690

TABLE 11

Measured values of flow parameters under post-critical conditions for PIB/D, 6%, $d = 1$ mm

$\bar{u}(0)/c$	l/d	L/d	D/d	$\bar{u}(L)/c$
0.8533	0.0000	1.9091	3.0909	0.0898
0.9656	0.0000	1.9091	3.0909	0.1011
1.1036	0.0000	1.9091	3.1818	0.1090
1.2875	0.0000	2.0000	3.3636	0.1138
1.4856	0.3636	2.1818	3.5455	0.1182
1.7557	1.1818	3.2727	3.8182	0.1204
2.1458	3.0909	5.0909	3.8182	0.1472
2.5750	5.4554	7.2727	3.4545	0.2158
2.7589	6.9091	8.2727	3.3636	0.2438
2.9711			2.4167	0.5087

(4) $M(L) < 1$ for all shock layer transitions.

(5) $M(L)$, D/d, $(L - l)/d$ decrease with d for each fixed l. The strength of the shock is greater in pipes of small diameter.

When the extrusion rates are high we get unsteady flow of fluids with large mean times of relaxation (Table 1) and smooth steady flow for fluids with small mean times of relaxation. When the degree of unsteadiness becomes too great, it is impossible to measure unique values of l/d, L/d and D/d. In certain periodic cases we can identify maximum and minimum values of these ratios over one cycle; in other cases, when the amplitude of oscillations is small, we record average values. Some photographs in which

TABLE 12

Measured values of flow parameters under post-critical conditions for PIB/D, 6%, $d = 1.57$ mm

$\bar{u}(0)/c$	l/d	L/d	D/d	$\bar{u}(L)/c$
0.3918	0.0000	1.1582	2.1424	0.0855
0.4477	0.0000	1.1582	2.1424	0.0975
0.5223	0.0000	1.2160	2.3162	0.0974
0.6268	0.0000	1.4476	2.4899	0.1011
0.7835	0.0000	1.5634	2.4899	0.1264
0.9794	0.0000	1.7950	2.8952	0.1168
1.1193	0.4054	2.0845	3.0110	0.1235
1.3058	1.2160	2.7215	2.9531	0.1497
1.5670	2.4899	4.0532	2.9531	0.1797
1.7411	3.5901	5.1534	2.8373	0.2163
1.9587	5.4430	6.6589	2.6636	0.2761
2.2385			2.3162	0.4172

TABLE 13

Measured values of flow parameters under post-critical conditions for PIB/D, 6%, $d = 2.08$ mm

$\bar{u}(0)/c$	l/d	L/d	D/d	$\bar{u}(L)/c$
0.2232	0.0000	0.7430	1.8357	0.0662
0.2551	0.0000	1.0926	1.8794	0.0722
0.2976	0.0000	1.0926	1.9231	0.0805
0.3571	0.0000	1.0926	1.9231	0.0966
0.4058	0.0000	1.0926	2.0105	0.1004
0.4960	0.0000	1.6213	2.1416	0.1081
0.6377	0.0000	1.6213	2.2727	0.1235
0.7440	0.0000	1.3986	2.4039	0.1287
0.8928	0.1311	1.5734	2.5787	0.1343
0.9920	0.3934	1.8357	2.6224	0.1442
1.1160	1.1581	2.3601	2.6224	0.1623
1.2754	1.6171	3.0157	2.6224	0.1855
1.4879	3.0157	4.4580	2.4913	0.2397
1.7855			2.0105	0.4417

the effects of unsteadiness is important are shown in Figs. 1.5 (a) and (b), 7.7 (a) and (b) and 7.14 (a) and (b). The values of $M(L)$ near one listed in Tables 6, 16 and 18 are inaccurate because the position of maximum swell is not stationary.

The case of steady flow at very high rates of extrusion in our experiments are characterized by smoothing the shock layer. In the more extreme cases the degree of smoothing is so great that the idea of a delay distance l is not

TABLE 14

Measured values of flow parameters under post-critical conditions for PIB/D, 6%, $d = 3.175$ mm

$\bar{u}(0)/c$	l/d	L/d	D/d	$\bar{u}(L)/c$
0.2554	0.0000	0.7731	1.4889	0.1152
0.2979	0.0000	0.9162	1.4889	0.1344
0.3575	0.0000	0.9449	1.5748	0.1442
0.4469	0.0000	0.9735	1.6607	0.1620
0.5959	0.0000	1.1739	1.7752	0.1891
0.7150	0.0000	1.2312	1.8898	0.2002
0.8938	0.2577	1.4603	2.0329	0.2163
1.0215	0.8590	1.9184	2.0329	0.2472
1.1172	0.9162	2.1761	2.0902	0.2557
1.1917	1.5462	2.8633	2.0043	0.2966
1.2768	1.5748	2.9492	1.9757	0.3271

TABLE 15

Measured values of flow parameters under post-critical conditions for PIB/D, 9.5%, $d = 1$ mm

$\bar{u}(0)/c$	l/d	L/d	D/d	$\bar{u}(L)/c$
1.4974	0.0000	1.7500	3.0830	0.1575
2.4957	0.0000	1.7500	3.3333	0.2246
3.7545	0.0000	2.2500	3.8333	0.2555
4.6795	0.0000	1.8333	3.8333	0.3185
4.9944	0.2500	1.8333	3.7500	0.3552
5.3511	0.2500	1.9170	3.8333	0.3642
5.7627	0.2500	2.1670	4.1670	0.3319
6.2466	0.8334	3.0830	4.1670	0.3597
6.8105	1.3333	3.8333	4.5000	0.3363
7.4959	2.0833	4.1670	4.5000	0.3702
8.3240	4.2503	6.1670	4.9170	0.3443
9.3753	5.7500	9.6670	3.9170	0.6111

useful. Examples of such smoothing can be seen in Figs. 7.13, 7.17, and in photographs shown in Section 8. Figures 8.1, 2, 3, 4(c) represent extreme cases of high speed extrusion without shock layers. The viscoelastic Mach

TABLE 16

Measured values of flow parameters under post-critical conditions for PIB/T, 4%, $d = 1$ mm

$\bar{u}(0)/c$	l/d	L/d	D/d	$\bar{u}(L)/d$
0.8042	0.0000	0.6429	1.6429	0.2979
0.8249	0.1429	0.7143	1.6429	0.3056
0.8356	0.2143	0.7143	1.6429	0.3096
0.8466	0.2143	0.8571	1.6429	0.3137
0.8579	0.2143	0.8571	1.6429	0.3178
0.8695	0.2143	0.9256	1.6429	0.3221
0.8814	0.2143	0.9256	1.6429	0.3266
0.8936	0.2857	1.0000	1.5714	0.3619
0.9062	0.3571	1.0714	1.5714	0.3670
0.9191	0.3571	1.1429	1.5714	0.3722
0.9325	0.4286	1.2857	1.5000	0.4144
0.9462	0.5000	1.3571	1.5000	0.4205
0.9603	0.5000	1.3571	1.5000	0.4268
0.9749	0.5714	1.3571	1.5000	0.4333
0.9898	0.5714	1.5000	1.5000	0.4399
1.0053	0.7143	1.5714	1.5000	0.4468
1.0213	0.8571	1.7143	1.5000	0.4539
1.0378	1.0714	1.7857	1.4286	0.5085
1.0723	1.6667	1.8333	1.6667	0.3860

TABLE 17

Measured values of flow parameters under post-critical conditions for PIB/T, 5.5%, $d = 1$ mm

$\bar{u}(0)/c$	l/d	L/d	D/d	$\bar{u}(L)/c$
1.1341	0.0000	0.7692	2.0769	0.2629
1.1813	0.0000	0.8462	2.0769	0.2738
1.2327	0.0000	0.9231	2.0769	0.2858
1.2601	0.1538	1.1538	2.0769	0.2921
1.3187	0.2308	0.9231	2.0769	0.3057
1.4176	0.2308	1.3077	2.1538	0.3056
1.5751	0.3077	1.4625	2.1538	0.3396
1.6677	0.5385	1.5385	2.0769	0.3867
1.8902	1.8462	2.6923	1.9231	0.5111

number ($M(L)$ is greater than one in all these cases. The type of complete smoothing which is exhibited in these figures may be general for high speed extrusion in the steady case.

The empty rows at the bottom of the columns in Tables 6–9 and 11–13 signal difficulties in defining and measuring the missing entry. Most of the entries in the last rows of the tables are "averages" over small amplitude oscillations and are not very accurate.

It is of definite interest to consider delayed die swell when the extrusion rates are high. The argument given at the end of Section 5 shows how high speed flow might be used to study hyperbolicity and change of type for

TABLE 18

Measured values of flow parameters under post-critical conditions for PIB/T, 6; $d = 1$ mm

$\bar{u}(0)/c$	l/d	L/d	D/d	$\bar{u}(L)/c$
2.2015	0.0000	1.000	2.3330	0.4045
2.3238	0.2500	1.1670	2.5000	0.3718
2.4605	0.3330	1.5830	2.5000	0.3937
2.6143	0.5830	1.7500	2.5000	0.4183
2.7886	0.8330	1.9170	2.5000	0.4462
2.9878	1.2500	2.4170	2.5000	0.4780
3.2176	2.0000	3.0000	2.4170	0.5508
3.4858	2.8330	3.6250	2.3330	0.6404
3.8027	3.0000	4.0000	2.2500	0.7511
4.1829	3.8750	4.9170	2.1670	0.8908
4.6477	a 3.1480	4.0000	2.2500	0.9181
	b –	7.2400	2.0800	1.0794

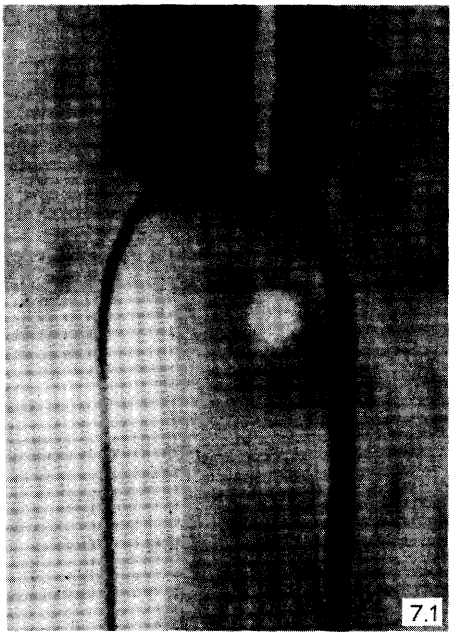

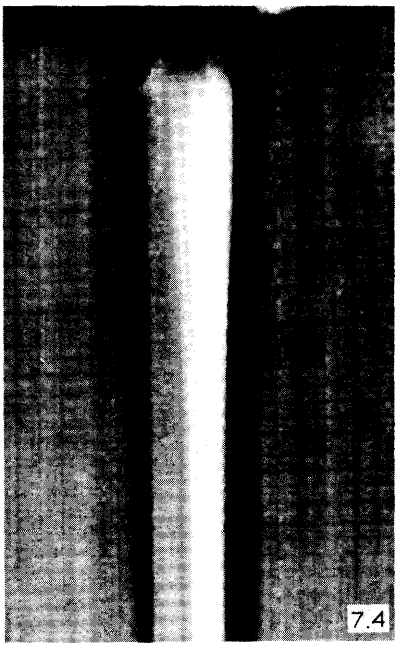

Fig. 7.1. Extrusion of PIB/D, 6% at criticality: $[d,\ \bar{u}(0)/c,\ M(L)] = [3.175\ \text{mm},\ 0.72,\ 0.20]$. The viscoelastic Mach number based on the maximum velocity at exit is 1.44.

Fig. 7.2. Extrusion of PIB/D, 6% under post-critical conditions: $[d,\ \bar{u}(0)/c,\ M(L)] = [3.175$ mm, 1.02, 0.247].

Fig. 7.3. Extrusion of PIB/D, 6% under post-critical conditions: $[d,\ \bar{u}(0)/c,\ M(L)] = [3.175$ mm, 1.28, 0.327].

Fig. 7.4. Extrusion of PIB/D, 6% at criticality: $[d,\ \bar{u}(0)/c,\ M(L)] = [1\ \text{mm},\ 1.29,\ 0.114]$.

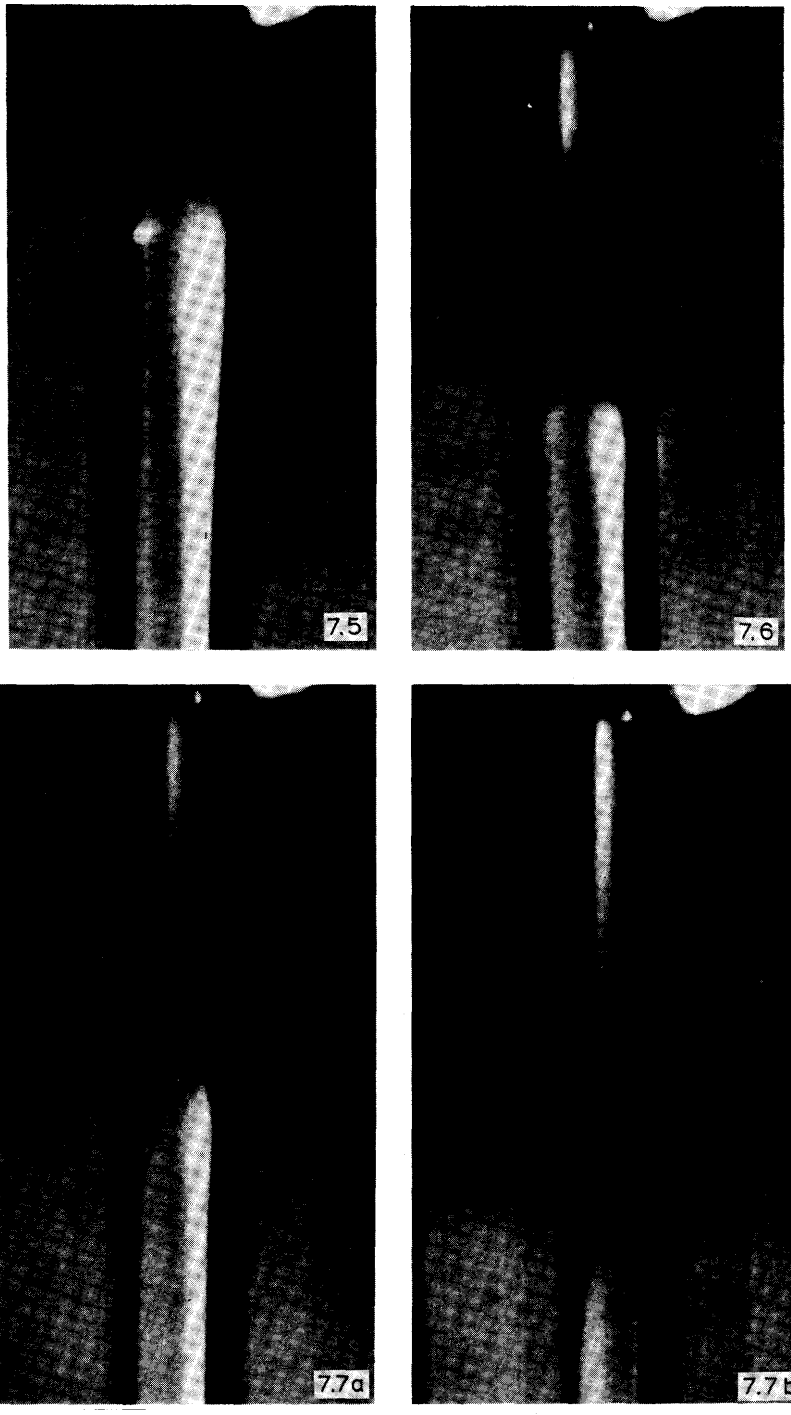

Fig. 7.5. Extrusion of PIB/D, 6% under post-critical conditions: $[d, \bar{u}(0)/c, M(L)] = [1\text{ mm}, 2.15, 0.147]$.

Fig. 7.6. Extrusion of PIB/D, 6% under post-critical conditions: $[d, \bar{u}(0)/c, M(L)] = [1\text{ mm}, 2.76, 0.244]$.

Fig. 7.7. Unsteady extrusion of PIB/D, 6% under terminal conditions: $[d, \bar{u}(0)/c] = [1\text{ mm}, 2.97]$. (a) shows the minimum delay distance over one cycle, (b) shows the maximum delay distance.

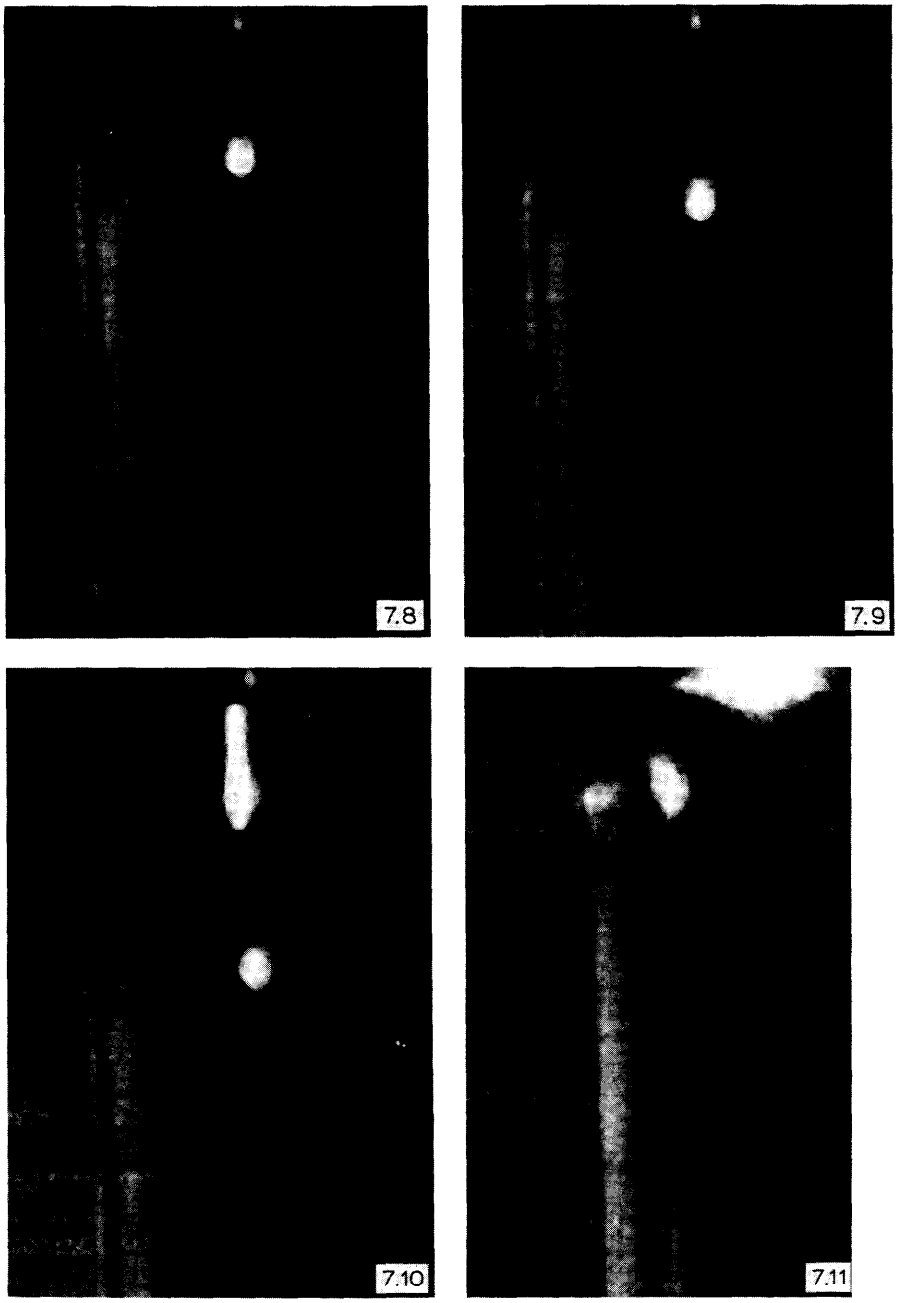

Fig. 7.8. Extrusion of CMC, 1.3% at criticality: $[d,\ \bar{u}(0)/c,\ M(L)] = [3.175$ mm, 0.477, 0.192].

Fig. 7.9. Extrusion of CMC, 1.3% under post-critical conditions: $[d,\ \bar{u}(0)/c,\ M(L)] = [3.175$ mm, 0.614, 0.224].

Fig. 7.10. Extrusion of CMC, 1.3% under post-critical conditions: $[d,\ \bar{u}(0)/c,\ M(L)] = [3.175$ mm, 0.716, 0.289].

Fig. 7.11. Extrusion of CMC, 1.3% at criticality: $[d,\ \bar{u}(0)/c,\ M(L)] = [1.57$ mm, 0.627, 016]. The viscoelastic Mach number based on the maximum velocity at exit is 1.254.

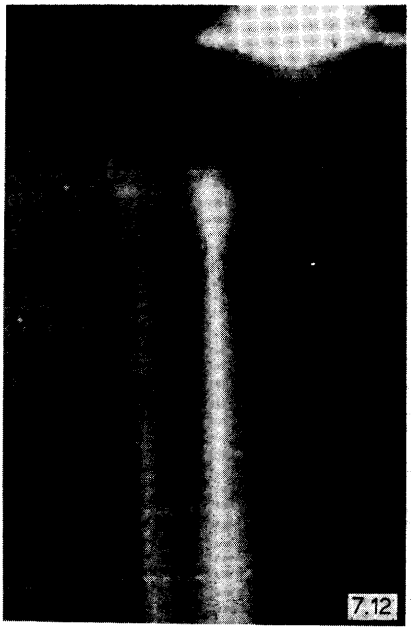

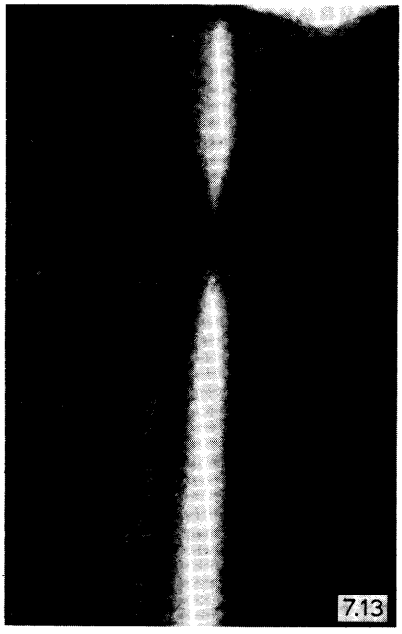

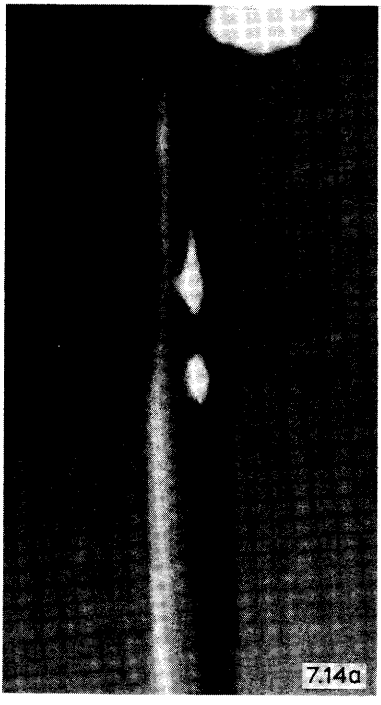

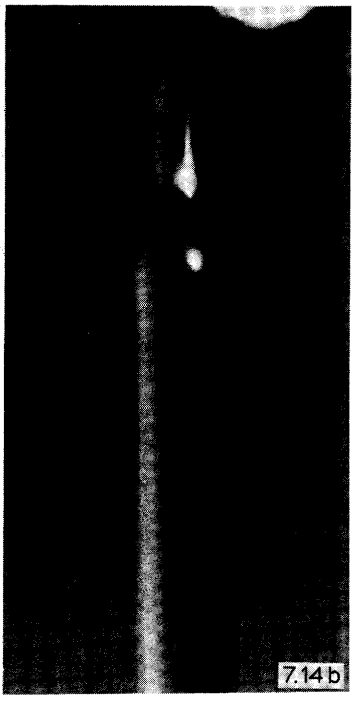

Fig. 7.12. Extrusion of CMC, 1.3% under post-critical conditions: $[d,\ \bar{u}(0)/c,\ M(L)] = [1.57$ mm, 0.798, 0.177].

Fig. 7.13. Extrusion of CMC, 1.3% under post-critical conditions: $[d,\ \bar{u}(0)/c,\ M(L)] = 1.57$ mm, 1.10, 0.497]. This figure shows how the delayed die swell is lost by smoothing at high extrusion rates.

Fig. 7.14. Unsteady response in extrusion of PIB/T, 6% under post-critical conditions: $[d,$ $\bar{u}(0)/c] = [1$ mm, 4.65]. (a) shows maximum delay, $[D/d,\ M(L)] = [2.08, 1.08]$, (b) shows minimum delay, $[D/d,\ M(L)] = [2.25, 0.9187]$.

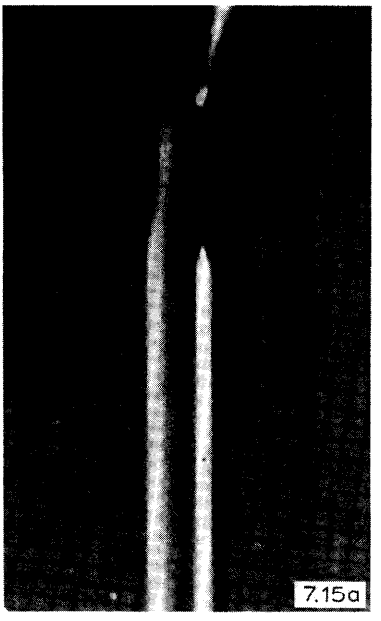

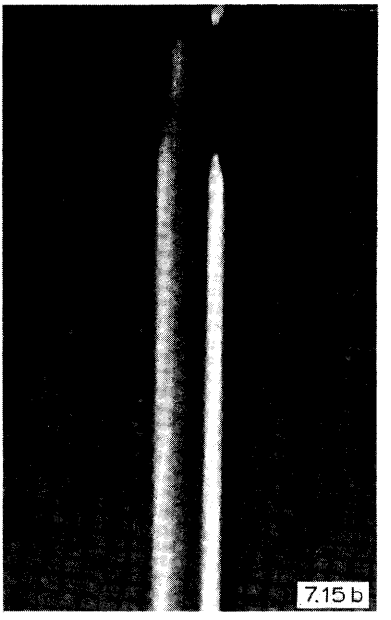

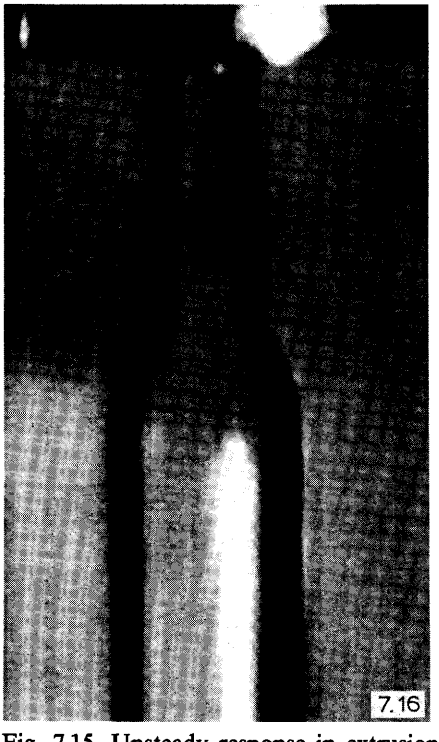

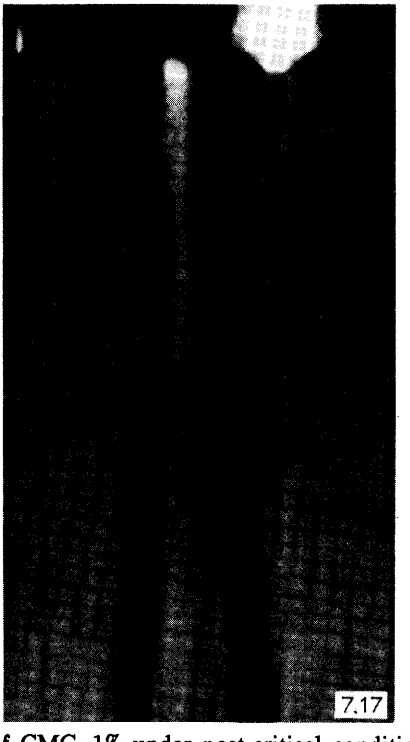

Fig. 7.15. Unsteady response in extrusion of CMC, 1% under post-critical conditions: $[d, \bar{u}(0)/c] = [1\text{ mm}, 3.74]$. (a) shows maximum delay, $[D/d, M(L)] = [1.75, 122]$. (b) shows minimum delay, $[D/d, M(L)] = [1.83, 1.10]$.

Fig. 7.16. Steady response in extrusion of PIB/D, 6% under post-critical conditions: $[d, \bar{u}(0)/c, M(L)] = [2.08\text{ mm}, 1.49, 0.240]$.

Fig. 7.17. Steady response in extrusion of PIB/D, 6% under post-critical conditions: $[d, \bar{u}(0)/c, M(L)] = [2.08\text{ mm}, 1.79, 0.442]$.

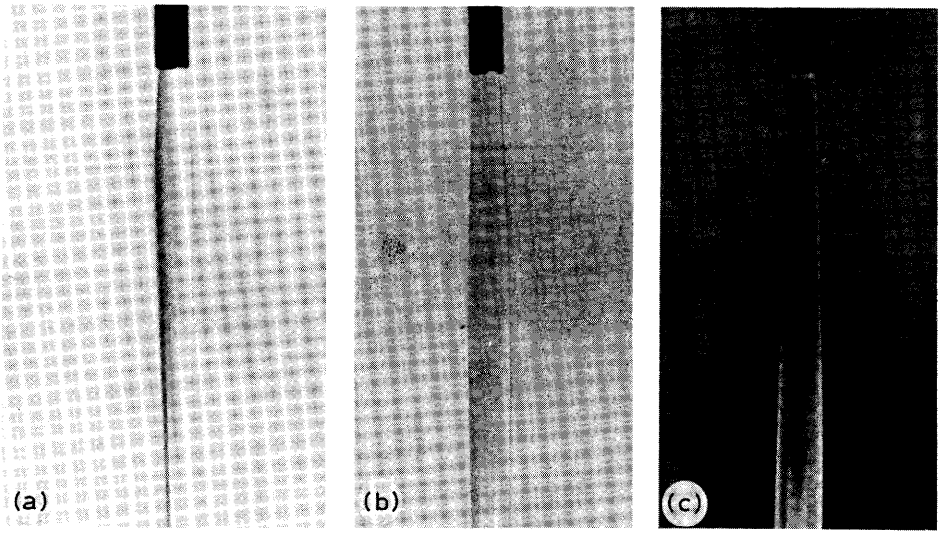

Fig. 8.1. Steady response of PIBM, 1% under post critical conditions: $[d, c] = [2.38$ mm, 18.8 cm/s], $[Q(\text{cm}^3/\text{s}), \phi(1/\text{s}), \bar{u}(0)/c, D/d, M(L)] =$ (a) [1.75, 1246, 2.73, 1.72, 0.923], (b) [2.13, 3757, 6.00, 1.68, 2.13], (c) [6.48, 5195, 8.30, 1.73, 2.77]. This fluid has a short time of relaxation, a relatively small viscosity and a Newtonian like response. There is a delayed swel but no "shock".

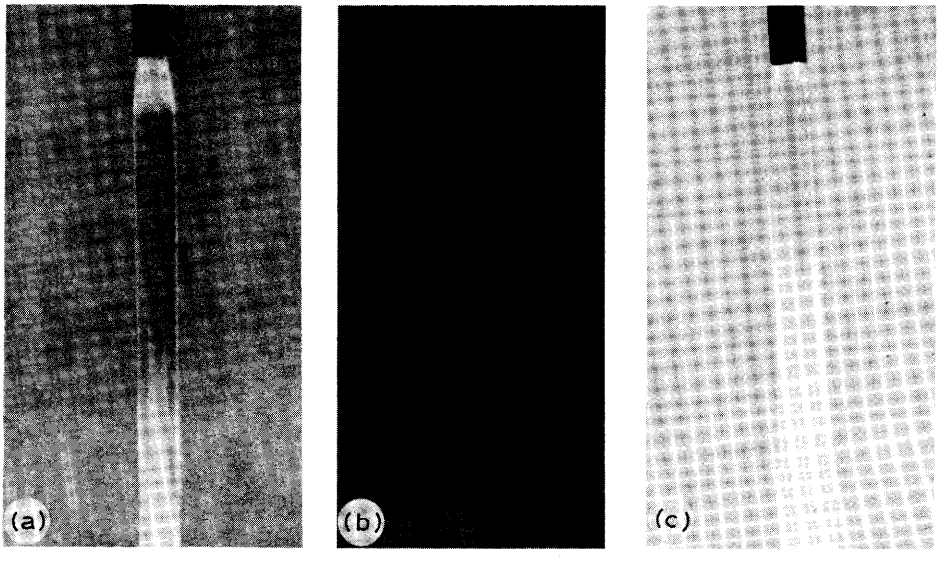

Fig. 8.2. Steady response of PMMA, 1% under post-critical conditions: $[d, c] = [2.38$ mm, 17.9 cm/s], $[Q(\text{cm}^3/\text{s}), \phi(1/\text{s}), \bar{u}(0)/c, D/d, M(L)] =$ (a) [2.13, 1708, 208, 1.62, 0.54], (b) [3.72, 2644, 4.41, 1.98, 1.15], (c) [4.68, 3757, 10.3, 2.15, 4.79]. This fluid is like the PIBM, 1% exhibited in figure 8.1.

delayed die swell. Unfortunately our extruding devices have a restricted speed capacity which set an upper limit on what we could study.

8. Post-critical dependence of the swell ratio on the shear rate and Reynolds number in fluids with a small mean time of relaxation

The four liquids with the shortest mean time of relaxation listed in Table 2 were studied in the Aberdeen laboratory of Dr. J. Matta before the Minnesota experiments were undertaken. These four liquids were the most Newtonian and the most stable of all those tested. The shape of the jets of these fluids is smoother and the flow is steadier than in more elastic fluids. The smooth shape may be the result of the action of an effective Newtonian viscosity associated with the rapid decay of the elastic response. The Aberdeen experiments were designed to determine the swell ratio as a function of the shear rate in the pipe and did not attempt to determine the critical condition for delay. Two of these fluids, Elavacite/9.8% and K-125/5% were also studied in Minnesota and critical conditions were determined.

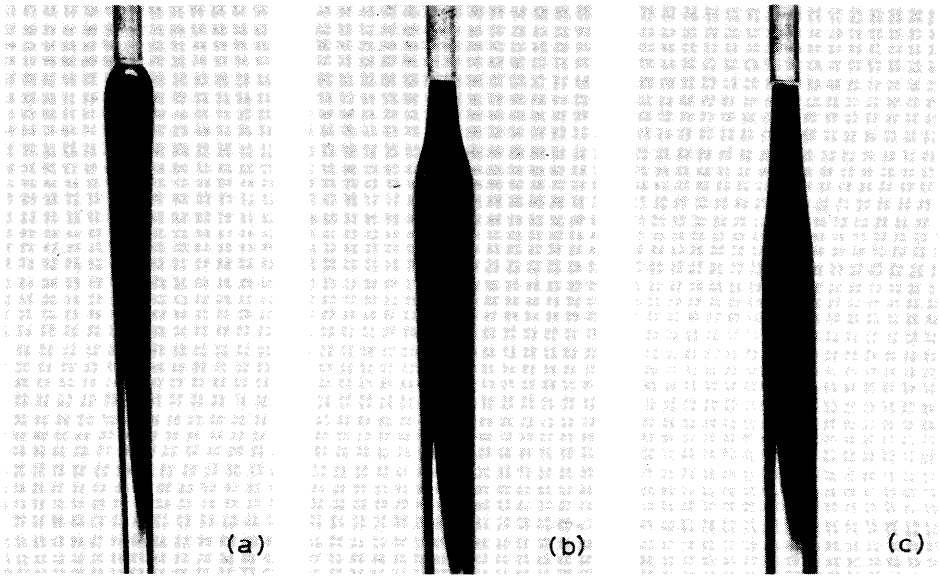

Fig. 8.3. Steady response of Elvacite, 9.8% under post-critical conditions: $[d, c] = [2.38$ mm, 67 cm/s], $[Q(\text{cm}^3/\text{s}), \phi(1/\text{s}), \bar{u}(0)/c, D/d, M(L)] =$ (a) [6.244, 4418, 1.97, 1.99, 0.50], (b) [20.1, 14283, 4.27, 2.43, 1.08], (c) [24.2, 17194, 5.14, 2.13, 1.69]. The Mach number $M(L) = \bar{u}(L)/c$ at the maximum swell is inferior to one when the maximum is achieved abruptly. Mach numbers $M(L)$ larger than one appear only after the shock has smoothed. This fluid has a short time of relaxation, but a larger viscosity than those shown in figures 8.1. and 8.2.

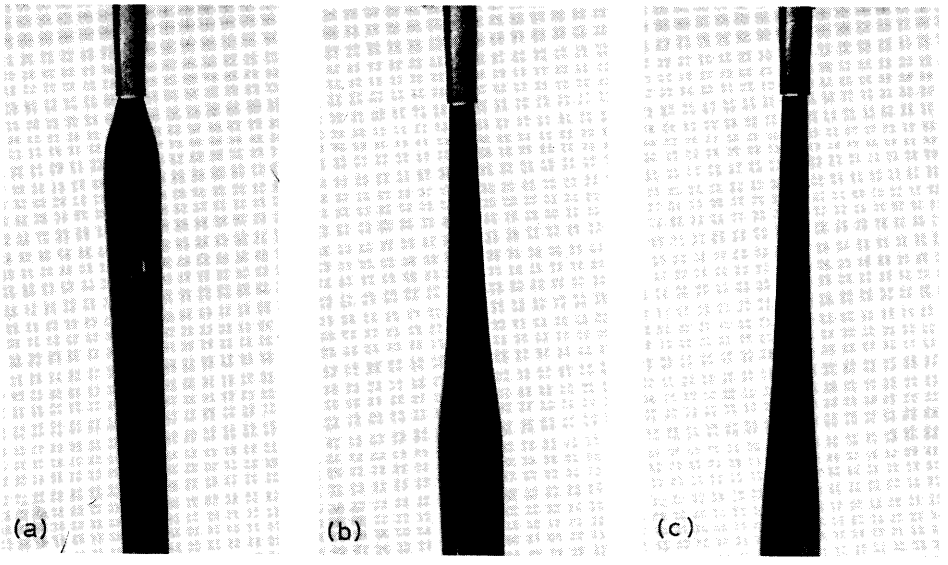

Fig. 8.4. Steady response of K-125, 5% under post-critical conditions: $[d, c] = [2.38$ mm, 45.5 cm/s], $[Q(\text{cm}^3/\text{s}), \phi(1/\text{s}), \bar{u}(0)/c, D/d, M(L)] =$ (a) [8.13, 5780, 3.8, 2.3, 0.72], (b) [21.5, 15360, 10, 2.6, 1.5], (c) [23.8, 16930, 11.1, 2.41, 1.92). The response of K-125, 5% is similar to Elvacite, 9.8%. The swell profile is "smooth" when $M(L) > 1$.

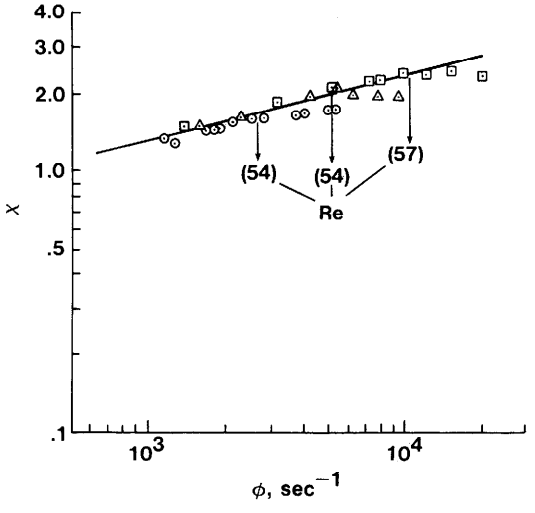

Fig. 8.5. Swell ratio $\chi = D/d$ as a function of the apparent rate of shear $\phi = 8\ \bar{u}(0)/d$ for PIBM/1% at $T = 24 \pm 1°$ C, $\odot = 2.39$ mm, $\triangle = 1.76$ mm and $\boxdot = 1.25$ mm. Figures 8.1 (a), (b) and (c) correspond, respectively, to $d = 2.39$ mm, $\phi = 1246$, $\phi = 3757$ and $\phi = 5195$.

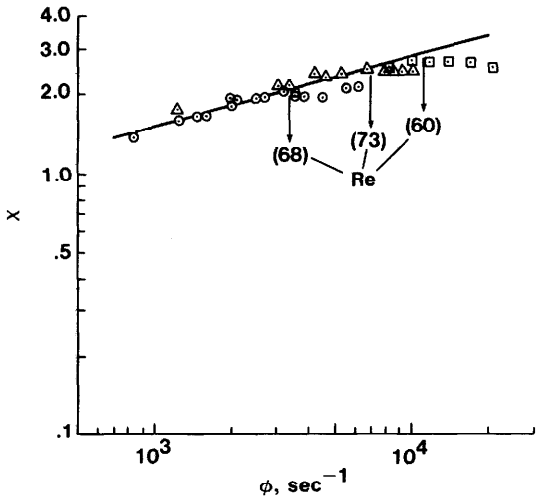

Fig. 8.6. Swell ratio $\chi = D/d$ as a function of the apparent rate of shear $\phi = 8\ \bar{u}(0)/d$ for PMMA/1% at $T = 24 \pm 1°C$, ⊙ = 2.39 mm, △ = 1.76 mm and ⊡ = 1.25 mm. Figures 8.2 (a), (b) and (c) correspond, respectively, to $d = 2.39$ mm, $\phi = 1708$, $\phi = 2644$ and $\phi = 3757$.

The results of the Aberdeen experiments are summarized in Figs. 8.5 through 8.8 where we have plotted the swell ratio D/d as a function of the shear rate ϕ with the nozzle diameter as a parameter. The straight lines in

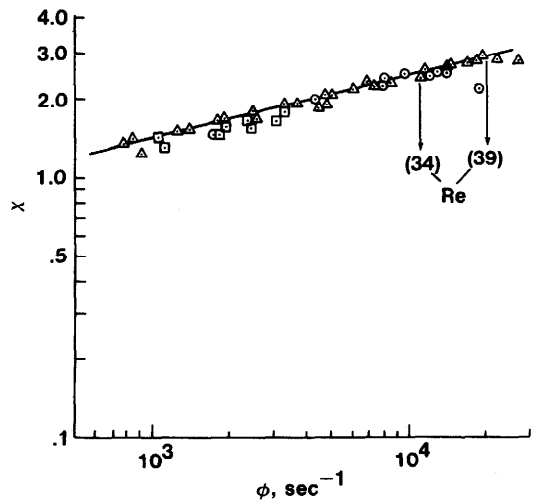

Fig. 8.7. Swell ratio $\chi = D/d$ as a function of the apparent rate of shear $\phi = 8\ \bar{u}(0)/d$ for Elvacite/9.8% at $T = 24 \pm 1°C$, ⊙ = 2.39 mm, △ = 1.76 mm and ⊡ = 1.25 mm. Figures 8.3 (a), (b) and (c) correspond, respectively, to $d = 2.39$ mm, $\phi = 4418$, $\phi = 14283$ and $\phi = 17194$.

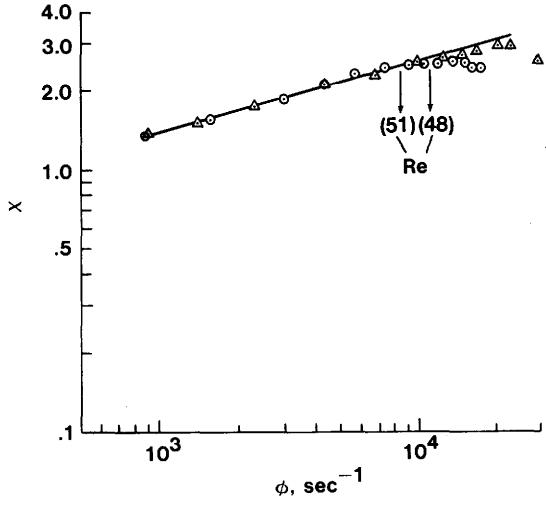

Fig. 8.8. Swell ratio $\chi = D/d$ as a function of the apparent rate of shear $\phi = 8\ \bar{u}(0)/d$ for K-125/5% as $T = 24 \pm 1°C$, ⊙ = 2.39 mm and ▲ = 1.86 mm. Figure 8.4 (a), (b) and (c) correspond, respectively, to $d = 2.39$ mm, $\phi = 5780$, $\phi = 15360$ and $\phi = 16930$.

the figures suggest that a power law expression exists between the swell ratio and the apparent shear rate $\phi = 8\bar{u}(0)/d$ that is independent of nozzle diameter. This may be expressed as $D/d = a\phi^b$ where a and b are constants dependent on material parameters of the fluid. At high shear rates, however, D/d begins to level out and eventually decreases with a further increase in the shear rate. The point of onset of this deviation is nozzle diameter dependent and occurs at lower shear rates for larger diameters. The Reynolds number, $R = \rho\bar{u}(0)d/\eta(\phi)$, using the shear dependent viscosity $\eta(\phi)$ at the current rate of shearing, at which the deviation becomes obvious, was determined, within limits, and indicated on each figure. The viscosities were deduced using standard capillary procedures and are consistent with lower shear rate cone and plate values. For a given fluid, the onset of deviation occurs roughly at the same Reynolds number for different nozzle diameters.

The effects of gravity and inertia may be important in the eventual decrease of the swell ratio. It is well known that inertia will decrease the swell ratio. This effect is more important at high than at low speeds. Gravity alone would eventually accelerate the jet to speeds greater than c and beyond with a constant decrease of the jet radius.

9. Conclusions

When a viscoelastic fluid is extruded from a pipe the diameter of the extruded jet usually increases. At low rates of extrusion the swell appears to

start at the pipe exit. At high rates of extrusion the tendency of the jet to swell at the exit is suppressed and there is a delay in the swell. This paper reports experimental results about the delay. We found that:

(1) Delayed die swell appears to be a general phenomenon. It occurred in each and every polymeric solution of the seventeen tested by us.

(2) Delayed die swell is a critical phenomenon. There is a definite critical extrusion velocity for the delay. When the extrusion velocity is greater than critical, there is a delay, a finite stand off before the major jet expansion.

(3) Delayed die swell occurred as a steady or unsteady response to steady extrusion, depending on the fluid. The response was unsteady in fluids with large mean times of relaxation and was steady for fluids with short mean times of relaxation.

(4) The critical extrusion velocity $\bar{u}_c$, the swell ratio D/d and the terminal swell distance L/d were decreasing functions of d, the pipe diameter.

(5) The critical Mach number at exit, $M_c = U_c/c$, $U_c = 2\bar{u}_c$, where c is the speed of vorticity waves into rest, was nearly always larger than one. (The value $M_c = 0.954$ for 1.3% CMC in a large pipe was the only exception.)

(6) There seems to be a limiting value of M_c for large values of d and the limit of M_c might be one.

(7) Whenever the die swell is delayed there are points r on the exit plane where $u(0, r) = c$.

(8) The critical terminal Mach number, after the swell $M(L) = \bar{u}(L)/c$, is definitely less than one. The post-critical case is defined by $\bar{u}(0) > \bar{u}_c$, $l > 0$.

The following facts hold in the post-critical case:

(9) $l > 0$ increases with $\bar{u}(0)$.

(10) $M_0 = 2\bar{u}(0)/c > 1$.

(11) $M(L) = \bar{u}(L)/c$ is an increasing function of $\bar{u}(0)$.

(12) $M(L) < 1$ for all shock layer transitions.

(13) $M(L)$, D/d, $(L-l)/d$ decrease with d for each fixed l. The strength of the shock is greater in pipes of small diameter.

(14) The response of fluids with moderate to long times of relaxation, $\lambda \geqslant 0.01$, became unsteady, perhaps time periodic, at some post-critical value of velocity less than terminal.

The following conclusions hold for large post-critical values of the extrusion velocity (the data taken here were restricted by limitations of the capacity of the extruder):

(15) The delayed die swell terminated in a large amplitude oscillation or by smoothing.

(16) Whenever the termination was stable, by smoothing, the shock layer of radius change was drastically smoothed and large values $M(L)$ could be

achieved for downstream. Conclusion (12) did not apply when the shock layer was suppressed.

(17) The smoothing occurred only in the four solutions with the smallest mean time of relaxation.

Acknowledgments

We wish to thank Professor G.S. Beavers for designing the constant displacement apparatus used in these experiments. The work of Joseph and Chen was supported by the U.S. Army, Mathematics and by the National Science Foundation, Fluid Mechanics.

References

1 D.D. Joseph, O. Riccius and M. Arney, Shear wave speeds and elastic moduli for different liquids; Part II. Experiments. (To appear in J. Fluid Mech., 1986).
2 M. Ahrens, J.Y. Yoo and D.D. Joseph, Hyperbolicity and change of type in the flow of viscoelastic fluids through pipes. J. Non-Newtonian Fluid Mech., 24 (1987) 67–83.
3 A.C. Merrington, Flow of viscoelastic materials in capillaries. Nature, London 152 (1943) 663.
4 H. Giesekus, Verschiedene phänonmene in Strömungen viskoelastischer Flüssigkeiten durch Düsen. Rheol. Acta, 8 (1968) 411–421.
5 A.B. Metzner, J.L. White and M.M. Denn, Behavior of viscoelastic materials in short time processes. Chemical Eng. Prog., 62 (1966) 81–92.
6 S. Middleman, The flow of high polymers. Interscience, 1968.
7 E. Brenschede and J. Klein. Bruckverluste und instabiles Fliessen elastischer Flussigskeiten im Hochdruck-Kappillarviskosimeter. Rheologica Acta, 9 (1970) 130–139.
8 D.D. Joseph, Hyperbolic phenomena in the flow of viscoelastic fluids, In: A.S. Lodge, J. Nohel and M. Renardy (Eds.), Viscoelasticity and Rheology, Academic Press, 1985.
9 B.D. Coleman and W. Noll, Foundations of linear viscoelasticity. Rev. Mod. Physics, 33 (1961) 239–249. Erratum, op. cit., 36 (1964) 1103.
10 J.C. Saut and D.D. Joseph, Fading memory, Arch. Rational Mech. Anal., 8 (1983) 53–95.
11 D.D. Joseph, M. Renardy and J.C. Saut, Hyperbolicity and change of type in the flow of viscoelastic fluids. Arch. Ration. Mech. Anal., 87 (1985) 213–251.
12 D.D. Joseph and J.C. Saut, Change of type and loss of evolution in the flow of viscoelastic fluids. J. Non-Newtonian Fluid Mech., 20 (1986) 117–141.
13 D.D. Joseph, A. Narain and O. Riccius, Shear wave speeds and elastic moduli for different liquids; Part I. Theory. (To appear in J. Fluid Mech., 1986).
14 I.M. Rutkevich, Some general properties of the equation of viscoelastic incompressible fluid dynamics. J. Appl. Math. Mech., 33 (1969) 42–51.
15 I.M. Rutkevich, The propagation of small perturbations in a viscoelastic fluid. J. Appl. Math. Mech., 34 (1970) 35–50.
16 J.S. Ultman and M.M. Denn, Anomalous heat transfer and a wave phenomenon in dilute polymer solutions. Trans. Soc. Rheology, 14 (1970) 307–317.
17 M. Luskin, On the classification of some model equations for viscoelasticity. J. Non-Newtonian Fluid Mech., 16 (1984) 3–11.

18 J.Y. Yoo, M. Ahrens and D.D. Joseph, Hyperbolicity and change of type in sink flow. J. Fluid Mech., 153 (1985) 203–214.
19 F. Dupret and J.M. Marchal, Loss of evolution in the flow of viscoelastic fluids. J. Non-Newtonian Fluid Mech., 20 (1986) 143–171.
20 J.Y. Yoo and D.D. Joseph, Hyperbolicity and change of type in the flow of viscoelastic fluids through channels. J. Non-Newtonian Fluid Mech., 19 (1985) 15–41.